2

Thermodynamic study of the phase separation mechanisms in nonstoichiometric Si oxide films during high temperature annealing

Andrey Sarikov*

IMDEA Materials Institute, C/ Eric Kandel, 2, 28906, Getafe, Madrid, Spain
V. Lashkarev Institute of Semiconductor Physics NAS Ukraine, 45 Nauki avenue, 03028, Kiev, Ukraine
*Corresponding author

Outline:

Introduction 37
Gibbs free energy of the Si / Si oxide systems 38
Equilibrium states in the Si / Si oxide systems 42
Si and Si oxide equilibrium within the concept of Si solubility in SiO_2 phase 45
Influence of the Si nanoinclusions / Si oxide matrix interfaces on the equilibrium states
during the phase separation of nonstoichiometric Si oxide films 47
Role of internal strain on the formation of equilibrium states in the
Si nanoinclusions / Si oxide systems 49
Conclusion 53
References 54

Introduction

Nonstoichiometric silicon oxide films (SiO_x, $x < 2$) are widely used for various applications such as protective and passivation layers [1], optical coatings [2], or insulating spacers [3] in contemporary electronic devices. Besides, perspective Si based nanoelectronic devices are discussed with composite structures consisting of nanometer sized amorphous or crystalline Si inclusions (nano-Si inclusions) embedded in Si oxide matrix, which are produced by high temperature phase separation of SiO_x films. The advantages of the nano-Si / Si oxide composites rely on their robustness and surface stability in comparison with porous materials as well as full process compatibility with complementary metal-oxide-semiconductor technology. Such structures have been suggested to use as light emitters [4-6] where efficient light emission in the visible spectral range is obtained due to the quantum confinement of charge carriers in the nano-Si particles [7]. Nanocrystalline Si inclusions embedded in SiO_2 matrix have been also proposed for the floating gates of flash memories with increased storage density and reduced power consumption [8-10]. Furthermore, the structures with nanosized Si can be used for the single electron memories and the spin-based quantum computation applications [11].

Nano-Si inclusions in Si oxide matrix are generally produced by high temperature annealing of nonstoichiometric silicon oxide films in inert atmosphere or in vacuum. Various methods have been used for the fabrication of initial SiO_x films such as Si ion implantation in SiO_2 [12, 13], co-sputtering [14-16] and electron beam co-evaporation [17] of Si and SiO, plasma enhanced chemical vapor deposition [18-22], molecular beam epitaxy [23], laser ablation [24, 25], and thermal vacuum or reactive evaporation of SiO [26-28]. Average size of nanosized Si precipitates can be controlled by either varying the annealing temperature or by changing the excess silicon content in the deposited nonstoichiometric SiO_x films. Reduction of oxygen content in SiO_x leads to the increased nano-Si precipitate size, density, and standard deviation of their distribution [29, 30]. Raising the annealing temperature also results in the increase of the average nano-Si size [31]. A higher level of flexibility is further provided by the superlattice approach suggested by Zacharias et al. [32], in which thin SiO_x layers alternate with stoichiometric SiO_2 layers not undergoing separation, so that the location, size (corresponding to the SiO_x layers thickness) and concentration of Si nanoinclusions in silicon oxide matrix can be defined independently.

During high temperature annealing, partial or complete decomposition of nonstoichiometric Si oxide takes place according to the following reaction:

$$x\, SiO_{x0} \rightarrow x_0\, SiO_x + (x - x_0)\, Si, \qquad 0 < x_0 < x \leq 2 \qquad (1)$$

where x_0 and x are the initial and the current stoichiometry indexes of the silicon oxide phase, respectively. Process (1) leads to the separation of the nano-Si precipitates and the increase of the oxygen concentration in the surrounding Si oxide matrix.

The degree of the phase separation of SiO_x films is often characterized by the equilibrium stoichiometry index of Si oxide matrix, x_{eq}, which also indicates the quantity of separated Si and, hence, the concentration and the average size of formed Si nanoinclusions. Experimental data show that $x_{eq} < 2$ (incomplete separation) for the annealing temperatures below about 950°C and increases with the increase of both x_0 and T values [33-36]. The degree of phase separation correlates with the amorphous or crystalline state of the nano-Si inclusions. For annealing temperatures not exceeding approximately 950°C mainly amorphous Si (a-Si) precipitates form, while at higher temperatures the formation of Si crystallites takes place, as revealed by Raman scattering data and high-resolution electron microscopy investigations [28, 37-42].

Understanding phase separation phenomenon in SiO_x films in terms of thermodynamics would enable to disclose the mechanisms guiding this process as well as to establish the basis for the macroscopic description of its kinetics. Thermodynamic approach requires to have the knowledge about the transformations of the Gibbs free energy in the Si / Si oxide systems during high temperature annealing. Minimum values of the Gibbs free energy of the mentioned systems determine the equilibrium between the silicon oxide and the separated Si as well as the equilibrium Si oxide composition.
At present, the comprehensive thermodynamic theory of the phase separation process in SiO_x films still remains a matter of investigations. To the best knowledge of us, La Magna et al. [43] were the first authors dealing explicitly with the Gibbs free energy of the separating Si oxide systems, introducing the expression for it in an empirical way. Although authors have explained some features of the process under study, in particular, the dependence of the final stoichiometry index of Si oxide on its initial value, their approach cannot be considered satisfactory from the physical point of view. In our earlier publication, we derived thermodynamically the expression for the Gibbs free energy of the Si oxide and the Si / Si oxide systems and studied the formation of equilibrium states between the bulk phases of amorphous or crystalline Si and Si oxide [44]. The expression for the Gibbs free energy [44] was later modified by addition of the strain component with empirical temperature dependence, in agreement with La Magna et al. [43], which enabled to reproduce the experimentally observed dependence of x_{eq} on the initial Si oxide stoichiometry and annealing temperature in the nano-Si inclusions / Si oxide matrix case [45, 46]. In this chapter, we present a consecutive and complete review of the thermodynamic study of the phase separation process of nonstoichiometric Si oxide films and the formation of the nanosized Si inclusions in silicon oxide matrix during high temperature annealing, based on our previous works devoted to this topic.

Gibbs free energy of the Si / Si oxide systems

From the thermodynamic point of view, a SiO_x film with $x < 2$ is a nonstable “kinetically frozen” system that evolves toward the equilibrium state during high temperature annealing. This evolution takes place by phase separation into Si and Si oxide with higher than initial index of stoichiometry, until the minimum value of the Gibbs free energy defining the formation of equilibrium between the separated phases, is reached.

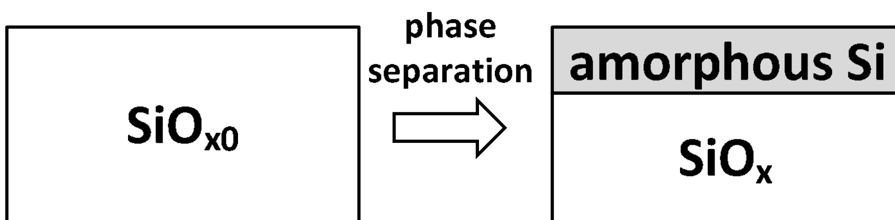

FIGURE 2.1
Geometry of the initial Si oxide and the phase separated amorphous Si / Si oxide system

Thermodynamic theory of equilibrium states in the systems composed of contacting Si and Si oxide phases has been proposed in our earlier publication [44]. Formation of equilibrium states is considered by the separation of excess Si atoms from the initial Si oxide with the stoichiometry index x_0 according to the reaction (1). As a first approximation, phase separation of SiO_{x0} film is assumed to form the contacting planar layers of Si and SiO_x as shown in Fig. 2.1, instead of the nanosized Si inclusions distributed in Si oxide matrix observed experimentally. Such simplified approach enables at the beginning not to take into account the contributions to the Gibbs free energy from the interfaces between the nano-Si inclusions and the surrounding Si oxide matrix. In addition, in the most general case we consider the separation of Si in amorphous state, while the Si oxide and the crystalline Si (c-Si) / Si oxide systems represent the partial cases.
The theory of the formation of equilibrium states operates with the total number of atoms (both silicon and oxygen), N_0, in the a-Si / Si oxide system. Using this quantity as well as the initial and the current stoichiometry indexes of Si oxide phase, the numbers of Si atoms separated in the amorphous Si phase, $N_{[Si]}^{a-Si}$, of Si atoms in the Si oxide phase, $N_{[Si]}^{SiOx}$, and of oxygen atoms, $N_{[O]}$, are expressed as follows:

$$N_{[Si]}^{a-Si} = N_0 \frac{x - x_0}{x(1 + x_0)}$$
$$N_{[Si]}^{SiOx} = N_0 \frac{x_0}{x(1 + x_0)} \qquad (2)$$
$$N_{[O]} = N_0 \frac{x_0}{1 + x_0}$$

The Gibbs free energy of the a-Si / Si oxide system is expressed as the sum of the contributions from both constituent phases as follows:

$$G = N_{[Si]}^{a-Si} g_{[Si]}^{a-Si} + G_{[SiOx]} \qquad (3)$$

Here, $g_{[Si]}^{a-Si}$ is the Gibbs free energy of a single Si atom in the amorphous Si phase and $G_{[SiOx]}$ is the Gibbs free energy of the Si oxide phase, respectively. We express the term $g_{[Si]}^{a-Si}$ with respect to the Gibbs free energy of a Si atom in the crystalline Si phase, $g_{[Si]}^{c-Si}$, in the following form [47]:

$$g_{[Si]}^{a-Si} = g_{[Si]}^{c-Si} + \frac{h_E - s_E T}{N_A} \qquad (4)$$

where h_E = 13400 J / mole is the molar crystallization enthalpy [48], s_E = 3.97 J / mole × K is the molar excess entropy of amorphous-to-crystalline transition [49], and $N_A = 6.022 \times 10^{23}$ mole^{-1} is the Avogadro constant, respectively.
The contribution to the Gibbs free energy from the SiO_x phase, $G_{[SiOx]}$, is expressed in the framework of the binary solution model [50] as follows:

$$G_{[SiOx]} = g_{[Si]} N_{[Si]}^{SiOx} + g_{[O]} N_{[O]} + \Delta G_{mix} \qquad (5)$$

where $g_{[Si]}$ and $g_{[O]}$ are the Gibbs free energies of the atoms of pure elements Si and O, respectively, and ΔG_{mix} is the change in the Gibbs free energy caused by intermixing these elements. The latter contribution is expressed in terms of a heat absorbed as a result of the formation of silicon oxide structure from the Si and O substances (enthalpy of mixing), ΔH_{mix}, and the difference in the entropy between the mixed and unmixed states (entropy of mixing), ΔS_{mix}, and looks as follows [50]:

$$\Delta G_{mix} = \Delta H_{mix} - T\Delta S_{mix} \tag{6}$$

The enthalpy of mixing is introduced here in a quasi chemical approach, i. e. it is assumed to arise due to the bond energies between adjacent atoms [50] In this view, the formation of silicon oxide phase occurs first by the breakage of $\frac{N_{[O]}}{2}$ O=O double bonds with the energy $\varepsilon_{O=O}$ and $2N_{[Si]}^{SiOx}$ Si–Si bonds with the energy ε_{Si-Si} so that one gets a positive contribution of $-\frac{N_{[O]}\varepsilon_{O=O}}{2} - 2N_{[Si]}^{SiOx}\varepsilon_{Si-Si}$ ($\varepsilon_{O=O}$, $\varepsilon_{Si-Si} < 0$). Heat is produced by the formation of $2N_{[O]}$ Si–O bonds with the bonding energy ε_{Si-O} and $2N_{[Si]}^{SiOx} - N_{[O]}$ Si–Si bonds with the bonding energy ε_{Si-Si} thus the negative contribution to the enthalpy of mixing results in $(2N_{[Si]}^{SiOx} - N_{[O]})\varepsilon_{Si-Si} + 2N_{[O]}\varepsilon_{Si-O}$.
Additional contribution to the enthalpy of mixing appears as a result of the microscopically inhomogeneous structure of silicon oxide phase. From the microscopic point of view, the nonstoichiometric silicon oxide is formed by the interconnected $Si{-}O_ySi_{4-y}$ tetrahedral units with different coordination numbers of the central Si atoms to the neighbouring silicon and oxygen atoms (y = 0, 1, 2, 3, 4) [51, 52]. The total number of units with all possible values of y is equal to the number of Si atoms in the silicon oxide phase, $N_{[Si]}^{SiOx}$. Considering random distribution of y between the $Si{-}O_ySi_{4-y}$ units, the probability to find either its value is calculated in the framework of the random bonding model proposed by Philipp [51]. The number of tetrahedral units with specific y in terms of quantities $N_{[Si]}^{SiOx}$ and $N_{[O]}$ is calculated as follows:

$$N_y = \frac{4!}{(4-y)!\,y!}\left(\frac{N_{[O]}}{2N_{[Si]}^{SiOx}}\right)^y \left[1 - \frac{N_{[O]}}{2N_{[Si]}^{SiOx}}\right]^{4-y} N_{[Si]}^{SiOx} \tag{7}$$

Hamann [53] as well as Bongiorno et al. [54] introduced the penalty energies of $Si{-}O_ySi_{4-y}$ tetrahedral units, Δ_y, as the measure of the energy nonequivalence of units with different oxidation degrees of central Si atoms ($\Delta_0 = \Delta_4 = 0$, Δ_1 = 0.5 eV, Δ_2 = 0.51 eV, Δ_3 = 0.22 eV) [54]. The contribution of $Si{-}O_ySi_{4-y}$ tetrahedral units to the enthalpy of mixing is obtained by multiplication of expression (7) by the respective value of Δ_y and summation over all possible values of y. The complete expression for ΔH_{mix} looks therefore as follows:

$$\Delta H_{mix} = N_{[O]}\varepsilon + N_{[Si]}^{SiOx}\sum_{y=0}^{4}\frac{4!}{(4-y)!\,y!}\left(\frac{N_{[O]}}{2N_{[Si]}^{SiOx}}\right)^y \left[1 - \frac{N_{[O]}}{2N_{[Si]}^{SiOx}}\right]^{4-y} \Delta_y \tag{8}$$

where $\varepsilon = 2\varepsilon_{Si-O} - \frac{\varepsilon_{O=O}}{2} - \varepsilon_{Si-Si}$.

Since the main contribution to the entropy of a solid solution is provided by its configuration part [55] the entropy of mixing of the SiO_x phase is calculated here as the configuration entropy associated with the arrangement of $N_{[O]}$ oxygen atoms among the $2N_{[Si]}^{SiOx}$ available places between the pairs of silicon atoms. According to [56], the following expression is realized:

$$\Delta S_{mix} = k_B \ln \frac{(2N_{[Si]}^{SiOx})!}{N_{[O]}! \times (2N_{[Si]}^{SiOx} - N_{[O]})!} \tag{9}$$

where $k = 1.38 \times 10^{-23}$ J / K is the Boltzmann's constant. This expression is simplified taking into account the Stirling's formula $n! \approx n \ln n - n$, which results in the following expression after all transformations:

$$\Delta S_{mix} = k_B \left(2N_{[Si]}^{SiOx} \ln \frac{2N_{[Si]}^{SiOx}}{2N_{[Si]}^{SiOx} - N_{[O]}} - N_{[O]} \ln \frac{N_{[O]}}{2N_{[Si]}^{SiOx} - N_{[O]}} \right) \tag{10}$$

Combination of formulas (3) to (10) enables to obtain the expression for the Gibbs free energy of a system consisting of the silicon oxide and the a-Si phases in the following form:

$$\begin{aligned} G = {} & N_{[Si]}^{a-Si} \left(g_{[Si]}^{c-Si} + \frac{h_E - s_E T}{N_A} \right) + g_{[Si]} N_{[Si]}^{SiOx} + g_{[O]} N_{[O]} + N_{[O]} \varepsilon + \\ & + N_{[Si]}^{SiOx} \sum_{y=0}^{4} \frac{4!}{(4-y)!\, y!} \left(\frac{N_{[O]}}{2N_{[Si]}^{SiOx}} \right)^y \left[1 - \frac{N_{[O]}}{2N_{[Si]}^{SiOx}} \right]^{4-y} \Delta_y - \\ & - k_B T \left(2N_{[Si]}^{SiOx} \ln \frac{2N_{[Si]}^{SiOx}}{2N_{[Si]}^{SiOx} - N_{[O]}} - N_{[O]} \ln \frac{N_{[O]}}{2N_{[Si]}^{SiOx} - N_{[O]}} \right) \end{aligned} \tag{11}$$

In the analysis, it is convenient to deal with the Gibbs free energy per one atom in the amorphous Si / Si oxide system, g, as a function of the initial and the current stoichiometry indexes of Si oxide, x_0 and x, respectively, and the temperature, T. The function $g = g(x_0, x, T)$ is obtained by dividing the expression (11) by the total number of atoms in the a-Si / SiO_x system, N_0, and substituting in it the expressions (2) for the quantities of silicon and oxygen atoms:

$$\begin{aligned} g(x_0, x, T) = \frac{G}{N_0} = \frac{x_0}{1 + x_0} \Bigg\{ & \left(\frac{1}{x_0} - \frac{1}{x} \right) \left[g_{[Si]}^{c-Si} + \frac{h_E - s_E T}{N_A} \right] + \\ & + \frac{g_{[Si]}}{x} + g_{[O]} + \varepsilon + \frac{1}{x} \sum_{y=0}^{4} \frac{4!}{(4-y)!\, y!} \left(\frac{x}{2} \right)^y \left[\frac{2-x}{2} \right]^{4-y} \Delta_y - \\ & - k_B T \left(\frac{2}{x} \ln \frac{2}{2-x} - \ln \frac{x}{2-x} \right) \Bigg\} \end{aligned} \tag{12}$$

Modification of expression (12) also enables to obtain the expressions for the Gibbs free energy per one atom in other related systems such as the Si oxide and the c-Si / Si oxide system. The former is achieved by setting $N_{[Si]}^{a-Si}=0$ (or $x = x_0$) and the latter by reduction of the term $\frac{h_E - s_E T}{N_A}$, respectively.

Analysis of the minimum values of expression (12) for the a-Si / Si oxide systems as well as the modified expression for the c-Si / Si oxide systems as the functions of annealing temperature and initial stoichiometry index of Si oxide phase enables to determine the equilibrium states (values of x_{eq}) of the mentioned systems. Instead of the Gibbs free energy $g(x_0, x, T)$, the reduced Gibbs free energy per one atom $g'(x_0, x, T)$ is introduced, the expression for which is obtained from the expression (12) truncating all the terms that are not functions of *x*. This is an admissible step in view of that the truncated terms influence only on the values of *g* and do not modify its behavior with respect to *x*. Besides, the equality $g_{[Si]} = g_{[Si]}^{c-Si}$ is set, which originates from the treatment of crystalline Si state as ideal crystal neglecting the small entropy contribution to $g_{[Si]}^{c-Si}$ [56]. The expression for the reduced Gibbs free energy of the amorphous Si / Si oxide system, $g'(x_0, x, T)$, looks therefore as follows:

$$g'(x_0,x,T)=\frac{x_0}{1+x_0}\left\{\frac{1}{x}\sum_{y=0}^{4}\frac{4!}{(4-y)!y!}\left(\frac{x}{2}\right)^{y}\left[\frac{2-x}{2}\right]^{4-y}\Delta_y - k_B T\left(\frac{2}{x}ln\frac{2}{2-x}-ln\frac{x}{2-x}\right)-\frac{1}{x}\frac{h_E-s_E T}{N_A}\right\} \tag{13}$$

The functions $g'(x_0, x, T)$ for the Si oxide and the crystalline Si / Si oxide systems are obtained by truncation of the last term in expression (13) for the latter case and by setting additionally $x = x_0$ for the former case, respectively.

Equilibrium states in the Si / Si oxide systems

The effects of the initial stoichiometry index of Si oxide phase, x_0, and the temperature on the evolution of the reduced Gibbs free energy of amorphous Si / SiO_x systems with the change of the current index of silicon oxide stoichiometry, *x*, are shown in Fig. 2.2. The data in Fig. 2.2 are shifted by $\frac{1}{1+x_0}\frac{h_E - s_E T}{N_A}$ with respect to the values (13) for better visualization. As can be seen from this figure, the theory predicts that the equilibrium states of a-Si / Si oxide systems, for which the Gibbs free energy has a minimum, correspond to incomplete phase separation in general case, i. e. to the values of the equilibrium stoichiometry of silicon oxide phase $x_{eq} < 2$. Analogous situation is obtained also for the c-Si / Si oxide systems, the only difference being higher values of x_{eq}.

The initial stoichiometry index of Si oxide phase is predicted to have no influence on the equilibrium silicon oxide composition in both amorphous (see Fig. 2.2(a)) and crystalline Si / Si oxide systems. Such conclusion can be also drawn from the mathematical analysis of expression (13). Indeed, the value of x_{eq} is obtained as a solution of the equation $\frac{\partial g'(x_0,x,T)}{\partial x}=0$ with respect

to x. This equation contains a certain function of x and T multiplied by $\frac{x_0}{1+x_0}$ in the left hand side. The latter term can be cancelled leaving therefore x and T the only equation parameters and making the solution independent on x_0.

Fig. 2.2(b) shows the calculated dependences of the reduced Gibbs free energy of amorphous Si / Si oxide systems on the stoichiometry index of Si oxide phase for different annealing temperatures. As the calculations demonstrate, the theory results in the negative effect of temperature on the equilibrium stoichiometry of silicon oxide in the a-Si / Si oxide as well as c-Si / Si oxide systems, i. e. the decrease of the values of x_{eq} with the increase of T. These conclusions are further supported by Fig. 2.3, in which the calculated temperature dependences of x_{eq} for both mentioned system types are presented.

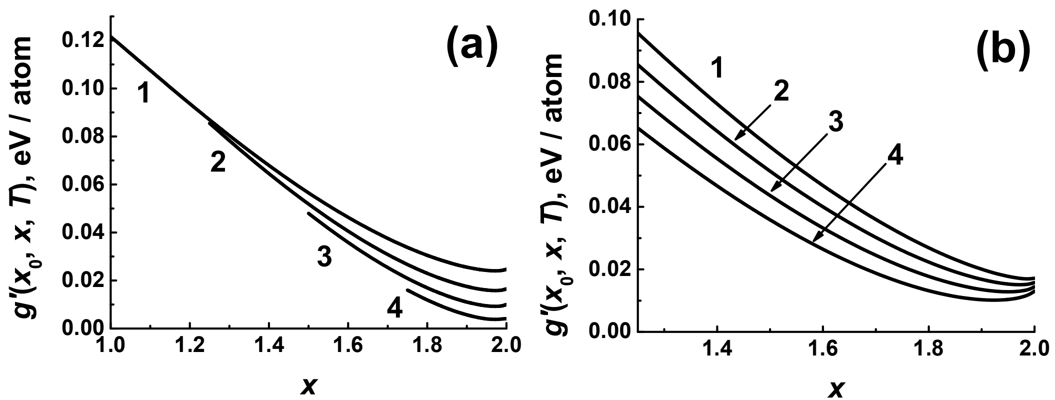

FIGURE 2.2

Dependence of the reduced Gibbs free energy on the Si oxide stoichiometry index in the a-Si / Si oxide systems:

(a) – for different initial stoichiometry indexes of Si oxide, x_0: 1 – 1, 2 – 1.25, 3 – 1.5, and 4 – 1.75, respectively. The annealing temperature is T = 800°C.

(b) – for different annealing temperatures, T: 1 – 600, 2 – 800, 3 – 1000, and 4 – 1200°C, respectively. The initial silicon oxide stoichiometry is x_0 = 1.25.

All values are shifted by $\frac{1}{1+x_0}\frac{h_E - s_E T}{N_A}$ with respect to the values (13) for better visualization

As follows from the thermodynamic model presented here, the evolution of nonstoichiometric silicon oxide films toward the separated Si / Si oxide states results from a combined action of several mechanisms described by separate terms in expression (13). The role of these mechanisms in promotion or suppression of the separation into silicon and silicon oxide phases is determined by whether their contributions to the Gibbs free energy of Si / Si oxide system descend or ascend with the increase of the value of stoichiometry index x. We analyze here all the participating mechanisms separately and disclose their effects on the phase separation process in nonstoichiometric silicon oxide films.

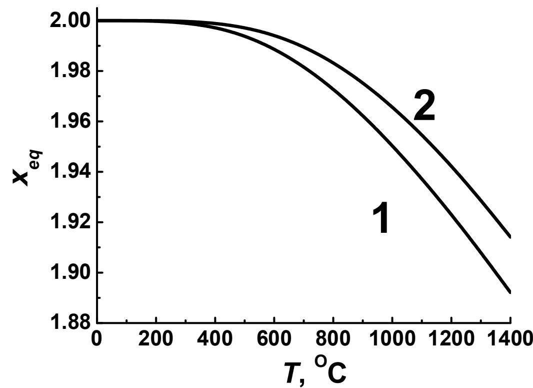

FIGURE 2.3
Calculated temperature dependences of the equilibrium stoichiometry indexes of Si oxide phase for the a-Si / Si oxide (1) and the c-Si / Si oxide (2) systems

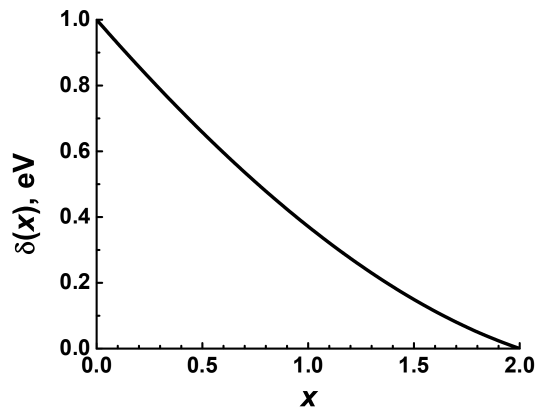

FIGURE 2.4
Contribution of the penalty energy of the $Si–O_ySi_{4–y}$ tetrahedral units of Si oxide phase to the Gibbs free energy of Si / Si oxide systems, $\delta(x)$, versus stoichiometry index of Si oxide phase, x

At the microscopic level, phase separation in nonstoichiometric Si oxide films takes place by local redistributions of oxygen atoms between the $Si–O_ySi_{4–y}$ tetrahedral units, composing the silicon oxide structure, so that oxygen is lost by the oxygen poor and gained by the oxygen rich units [57-59]. The exothermic character of the local disproportionation leading to the increase in the difference between the oxidation degrees of central Si atoms in the neighboring $Si–O_ySi_{4–y}$ tetrahedra has been also demonstrated theoretically by small cluster model quantum mechanical calculations [60, 61]. In terms of the penalty energy of $Si–O_ySi_{4–y}$ tetrahedral units, the local disproportionation results in the decrease of the total penalty energy of participating units. The decrease in the penalty energy of entire Si / Si oxide system with the progress of phase separation (increase of the value of x) leads to the decrease of respective contribution to the Gibbs free energy, $\delta(x)=\frac{1}{x}\sum_{y=0}^{4}\frac{4!}{(4-y)!\,y!}\left(\frac{x}{2}\right)^{y}\left[\frac{2-x}{2}\right]^{4-y}\Delta_y$, as demonstrated in Fig. 2.4. The tendency to minimize the total penalty energy of Si / Si oxide system is therefore a driving force for the

transformation of initial nonstoichiometric silicon oxide state in the separated Si and SiO_x phases. As can be seen in Fig. 2.4, the minimum value of $\delta(x)$ equal to zero is obtained for $x = 2$ corresponding to the complete separation in the stoichiometric Si and SiO_2 phases. This result is supported by van Harpert et al. [62] who considered the discussed mechanism alone and deduced the equilibrium state of Si / Si oxide systems in form of coexisting Si and SiO_2 phases as providing zero total penalty energy of all the $Si–O_ySi_{4–y}$ tetrahedral units.

The separation of Si and Si oxide is accompanied also by the transformation of the configuration entropy of Si / Si oxide system. The entropy value decreases with the increase in the value of x due to the reduction of the number of possible Si / Si oxide configurations (number of the arrangements of oxygen atoms between the pairs of silicon atoms in the silicon oxide phase). Such entropy behavior results in the increase of the respective contribution to the Gibbs free energy, which is demonstrated by the positive values of its derivative with respect to x proportional to $\frac{1}{x^2} ln \frac{2}{2-x} > 0$. Some more one Gibbs free energy term increasing with x is provided for the a-Si / Si oxide systems by the separation of amorphous Si phase (see expression (13)). The mechanisms behind both processes considered suppress therefore the phase separation in nonstoichiometric Si oxide films and promote the conservation of the stoichiometry index of silicon oxide phase at the initial value.

Combined action of the mechanisms promoting and suppressing the phase separation process in nonstoichiometric silicon oxide films during high temperature annealing results in the equilibrium states in them corresponding to incomplete Si and Si oxide separation, and the values of the equilibrium silicon oxide stoichiometry $x_{eq} < 2$. This situation is shown in Figs. 2.2 and 2.3 above. As can be seen from the expression (13), the dependence of x_{eq} on the temperature is determined by only the suppressing mechanisms, the contributions of which to the Gibbs free energy of Si / Si oxide systems are the ascending functions of x. The values of these contributions increase with the growth of temperature that makes x_{eq} shift toward smaller values, as demonstrated by the results presented in Figs. 2.2(b) and 2.3. The lower values of x_{eq} in the a-Si / Si oxide systems as compared to the c-Si / Si oxide case originate from the additional ascending with x contribution to the Gibbs free energy from the separated a-Si phase, as will be discussed in more detail below.

Si and Si oxide equilibrium within the concept of Si solubility in SiO_2 phase

The equilibrium states in the Si / Si oxide systems can now be analyzed in terms of the excess Si concentration in the silicon oxide considering the SiO_x phase as the stoichiometric SiO_2 with excess Si dissolved in it. The equilibrium value of excess Si concentration corresponds to the solubility limit of Si in SiO_2. The independence of the equilibrium stoichiometry index of Si oxide phase on the value of x_0 as well as its decrease with the increase of temperature (see Figs. 2.2 and 2.3) comply with the solubility limit concept. Whatever is the initial composition of silicon oxide phase, the equilibrium Si concentration in silicon oxide in excess to that in SiO_2 does not depend on it and is determined by only the temperature (grows with the temperature) and the structure of Si phase.

Temperature dependences of the solubility limits of Si in SiO_2 in the a-Si / SiO_x and c-Si / SiO_x systems can be calculated from the data for x_{eq} presented in Fig. 2.3. Taking into account the relations (2), the Si concentration in SiO_x phase is calculated as $C_{[Si]}^{SiOx} = \frac{C_0}{1+x}$, where $C_0 \approx 7 \times 10^{22}$

cm^{-3} is the total estimated concentration of atoms in the nonstoichiometric silicon oxide [43]. The Si concentration in stoichiometric SiO_2 is therefore equal to $C_{[Si]}^{SiO2} = \frac{C_0}{3}$ and the equilibrium Si concentration in silicon oxide to $C_{[Si]}^{SiOxeq} = \frac{C_0}{1+x_{eq}}$, respectively. The equilibrium Si concentration in the nonstoichiometric silicon oxide with composition x_{eq} in excess to that in SiO_2 phase, i. e. the solubility limit of Si in SiO_2 can be calculated now as $\Delta C_{[Si]} = C_{[Si]}^{SiOxeq} - C_{[Si]}^{SiO2} = C_0 \frac{2-x_{eq}}{3(1+x_{eq})}$. The temperature dependences of the solubility limits of Si in SiO_2 in contact with both amorphous and crystalline Si, obtained by this expression, are shown in Fig. 2.5 in coordinates ln $\Delta C_{[Si]}$ vs. T^{-1}, in which they are linearized. The functions $\Delta C_{[Si]}(T)$ may be described therefore by the traditional Arrhenius dependences for the solubility limits, $\Delta C_{[Si]} = \Delta C_{[Si]}^0 \times exp\left(-\frac{E_{sol}}{k_B T}\right)$, where $\Delta C_{[Si]}^0$ is the pre-exponential factor and E_{sol} is the activation energy of dissolution, respectively. The characteristics of the dissolution process of Si in SiO_2 in contact with both amorphous and crystalline Si are obtained by linear fits of the calculated values of $\Delta C_{[Si]}$ in Fig. 2.5 and are shown in Table 2.1.

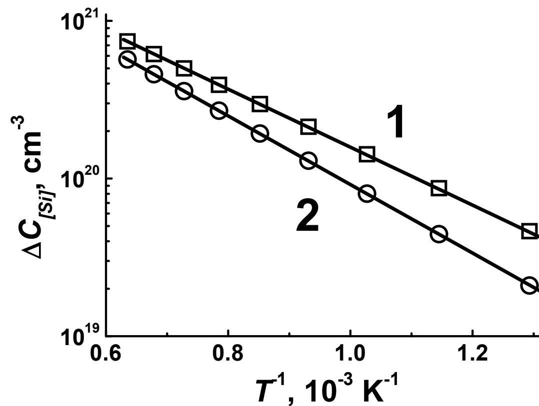

FIGURE 2.5
Dependence of the solubility limit of Si in SiO_2 phase on the inverse temperature for the a-Si / Si oxide (1) and the c-Si / Si oxide (2) systems. Symbols present the results of calculations by the expression $\Delta C_{[Si]} = C_0 \frac{2-x_{eq}}{3(1+x_{eq})}$ and lines are the approximations by Arrhenius dependences in the form $\Delta C_{[Si]} = \Delta C_{[Si]}^0 \times exp\left(-\frac{E_{sol}}{k_B T}\right)$, respectively

TABLE 2.1
Characteristics of the solubility of Si in SiO_2 in contact with amorphous and crystalline Si phases

	$\Delta C_{[Si]}^0$, cm^{-3}	E_{sol}, eV
amorphous Si	1.09×10^{22}	0.36
crystalline Si	1.37×10^{22}	0.43

Calculated temperature dependences of the solubility limits of Si in SiO_2 are at the best to be compared with respective experimental results. However, the information about the solubility limits of Si in SiO_2 is lacking [63]. Agarwal and Dunham [64] estimated the solubility concentration of Si in SiO_2 to be ~ 4×10^{20} cm^{-3} at 1100°C, which is close to the value ~ 3.5×10^{20} cm^{-3} obtained in our study for SiO_2 in contact with crystalline Si at this temperature. The solubility limit of Si in SiO_2 in contact with amorphous Si is higher due to the higher value of the Gibbs free energy of Si atoms in a-Si phase (chemical potential) by $\frac{h_E - s_E T}{N_A}$ (see expression (4)). Equilibrium between the Si and the Si oxide means equalizing the chemical potentials of Si in both phases. Therefore, more Si atoms tend to dissolve in equilibrium from amorphous Si into SiO_2 leading to higher solubility limits and lower values of equilibrium silicon oxide stoichiometry than those for the crystalline Si / SiO_2 systems. The function $\frac{h_E - s_E T}{N_A}$ decreases with the temperature therefore reducing the relative driving force of Si dissolution from the a-Si state compared to that from the c-Si and leading to smaller value of the activation energy of Si solubility for this case.

Influence of the Si nanoinclusions / Si oxide matrix interfaces on the equilibrium states during the phase separation of nonstoichiometric Si oxide films

As mentioned above, the results of experimental investigations of the process of phase separation in nonstoichiometric Si oxide films indicate the increase of the equilibrium stoichiometry index of Si oxide with the increase of both the initial stoichiometry index [28, 43] and the annealing temperature [33-36]. At the same time, the theoretical results described in the previous sections show the predicted independence of the equilibrium value of x_{eq} on the initial Si oxide composition as well as its decrease when the annealing temperature increases (see Figs. 2.2 and 2.3). It is obvious therefore that the theory of the formation of equilibrium states in the Si / Si oxide systems requires modification and account of additional acting mechanisms to enable to explain the experimentally observed features during the phase separation of SiO_x films.
One of the mechanisms that may presumably affect the SiO_x phase separation is the formation of the interfaces of nano-Si inclusions with surrounding Si oxide matrix. The relative area of such interfaces is high enough in view of the small nano-Si sizes so that the interface free energy may possibly have an influence on the value of x_{eq} and its dependence on the annealing temperature.
The contribution to the Gibbs free energy related to the formation of nano-Si / Si oxide interfaces may be estimated in the following way. Setting $f(r)$ to be the distribution function of the nano-Si inclusions on radius, this contribution is expressed as follows:

$$G_{interface} = 4\pi\gamma N_{pre} \int_0^{\infty} r^2 f(r) dr \qquad (14)$$

where γ is the energy of the unit area of the nano-Si / Si oxide interface and N_{pre} is the total quantity of Si precipitates formed by the phase separation of nonstoichiometric Si oxide film with the total number of atoms N_0, respectively.

When, for simplicity, all the nano-Si inclusions are considered to have the same average radius R, the interface contribution to the Gibbs free energy per one atom in the nano-Si / Si oxide system looks as follows:

$$g_{interface} = 4\pi\gamma R^2 \frac{N_{pre}}{N_0} \tag{15}$$

where the radius of the nano-Si inclusions is expressed as a function of the initial and current stoichiometry index of Si oxide matrix in the following way:

$$R = \sqrt[3]{\frac{3\Omega}{4\pi} i} = \sqrt[3]{\frac{3\Omega}{4\pi} \frac{N_{[Si]}^{a-Si}}{N_{pre}}} = \sqrt[3]{\frac{3\Omega}{4\pi} \frac{x - x_0}{x(1+x_0)} \frac{N_0}{N_{pre}}} \tag{16}$$

Here, $\Omega \approx 2.29 \times 10^{-29}$ m^3 is the volume per one Si atom in the Si phase [65] and i is the number of Si atoms in a single nanoinclusion, respectively.
The estimations of the influence of the interfaces of the Si nanoinclusions with Si oxide matrix on the Gibbs free energy values have been performed for the case of the formation of amorphous Si inclusions taking place at the temperatures between about 600 to 950°C, as reported above [28, 37-42]. In relation to this, the value of the specific interface energy γ, according to the data of [66], was accepted equal to 0.01 J / m^2. Indicated temperature range is the most important for the investigations because it corresponds to the main temperature dependence of the equilibrium stoichiometry index of Si oxide matrix [33, 34]. The values of $\frac{N_{pre}}{N_0}$ are calculated from the ratios of respective concentrations, $\frac{C_{pre}}{C_0}$, referring to the typical concentrations of Si nanoinclusions C_{pre} of about 10^{18} cm^{-3} [67, 68].
Fig. 2.6 shows the dependences of the $g_{interface}$ calculated by expression (15) on the stoichiometry index of SiO_x matrix for different values of the initial Si oxide stoichiometry x_0 as well as for different nano-Si concentrations. It can be seen from this figure that the contribution to the Gibbs free energy from the a-Si / Si oxide interfaces does not exceed the values of approximately 5×10^{-4} eV / atom for reasonable C_{pre} values, which is at least two orders of magnitude smaller than the data presented in Fig. 2.2. Partial crystallization of amorphous Si nanoinclusions may lead to the modification of the effective value of γ by about one order of magnitude (γ is equal 0.1 to 0.6 J / m^2 for the bulk c-Si / SiO_2 interface [69-71]), which will result in the proportional change of the value of the contribution of interface between the Si nanoinclusions and Si oxide matrix. This will not lead, however, to a significant modification of the values of g' expressed as the sum of the expressions (13) and (15). Moreover, multiple studies, despite differences in mathematical representations, demonstrate the decrease of the interface free energy of nanoparticles with the decrease of their sizes [72-74], which leads to additional decrease of the value of the contribution to the Gibbs free energy from the nano-Si / Si oxide interfaces.

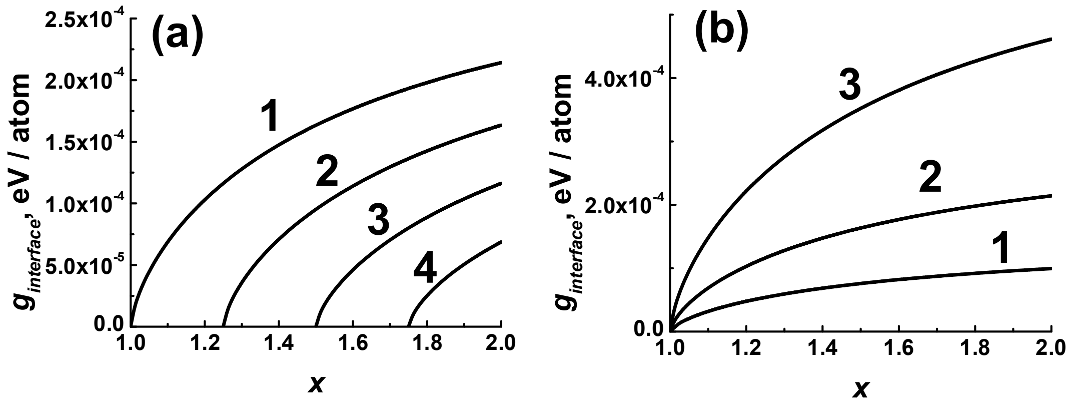

FIGURE 2.6
Dependence of the nano-Si / Si oxide interface contribution to the Gibbs free energy on the Si oxide stoichiometry index in the a-Si / Si oxide systems:
(a) — for different initial stoichiometry indexes of Si oxide, x_0: 1 – 1, 2 – 1.25, 3 – 1.5, and 4 – 1.75, respectively. C_{pre} = 10^{18} см$^{-3}$.
(б) — for different nano-Si concentrations, C_{pre}: 1 – 10^{17}, 2 – 10^{18}, and 3 – 10^{19} cm^{-3}, respectively. The initial silicon oxide stoichiometry is x_0 = 1

This indicates that the formation of the interfaces between the formed Si nanoinclusions and surrounding silicon oxide matrix during the phase separation of nonstoichiometric Si oxide films should be considered as a factor with minor importance for the establishment of the equilibrium states in the nano-Si / Si oxide systems.

Role of internal strain on the formation of equilibrium states in the Si nanoinclusions / Si oxide systems

From the mathematical point of view, to agree the theoretical and experimental results on the influence of the temperature and the value of x_0 on the nano-Si / Si oxide matrix equilibrium, the expression (13) should be extended with at least one term corresponding to the mechanism suppressing the Si and Si oxide separation. The mathematical structure of this additional term should meet the following requirements [45]:

(a) superlinear dependence on the difference between the current and the initial stoichiometry indexes of Si oxide phase, to be able to reproduce the increase of the value of x_{eq} with the increase of x_0 value;

(b) descending dependence on the annealing temperature, so that the shift of the minimum Gibbs free energy of nano-Si / Si oxide system toward smaller x with the raise of temperature would be enabled.

First requirement is met by the expression for the contribution to the Gibbs free energy of nonstoichiometric Si oxide arising due to the internal strain that appears as a result of the atom redistribution during the phase separation, introduced in the following form in [43, 75]:

$$\Delta g_{SiOx}(x_0, x) = \frac{1}{2} E\left[\varepsilon_0 (x - x_0)\right]^2 \qquad (17)$$

Here, $\Delta g_{SiOx}(x_0, x)$ is the density of the strain related Gibbs free energy of silicon oxide, E = 70 GPa is the Young's modulus of Si oxide, $\varepsilon_0 = \frac{1}{a}\frac{\partial a}{\partial x}$ is the composition extension coefficient, and a is the average distance between the atoms in the system under consideration, respectively. Authors [43] have modified the phenomenological expression for the Gibbs free energy density of SiO_x films with the term (17) and explained qualitatively the dependence of the equilibrium stoichiometry index of phase separated silicon oxide on its initial value (see Fig. 2.7). At this, however, no quantitative comparison with experimental data as well as no temperature dependence of the contribution Δg_{SiOx} has been provided.

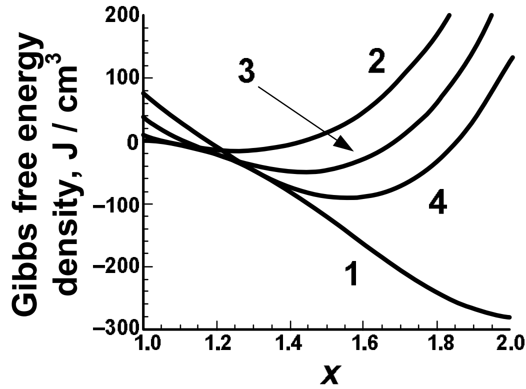

FIGURE 2.7
Dependences of the Gibbs free energy density of the nonstoichiometric Si oxide on its composition without internal strain (1) as well as with strain account for different values of the initial Si oxide stoichiometry, x_0: 2 – 1.1, 3 – 1.2, and 4 – 1.3, respectively. The values of the stoichiometry index in minimums: 2 – 1.26, 3 – 1.43, and 4 – 1.55, respectively (according to [43])

We consider the strain contribution to the Gibbs free energy per one atom (13) of the Si / Si oxide system by analogy with expression (17) but in general form, using a temperature dependent function $\chi(T)$ as follows [45]:

$$\Delta g_{strain}(x_0, x, T) = \chi(T)(x - x_0)^2 \qquad (18)$$

so that the expression (13) transforms into

$$g'(x_0, x, T) = \frac{x_0}{1+x_0}\left\{\frac{1}{x}\sum_{y=0}^{4}\frac{4!}{(4-y)!\,y!}\left(\frac{x}{2}\right)^{y}\left[\frac{2-x}{2}\right]^{4-y}\Delta_y - kT\left(\frac{2}{x}ln\frac{2}{2-x} - ln\frac{x}{2-x}\right) - \frac{1}{x}\frac{h_E - s_E T}{N_A}\right\} + \chi(T)(x - x_0)^2 \qquad (19)$$

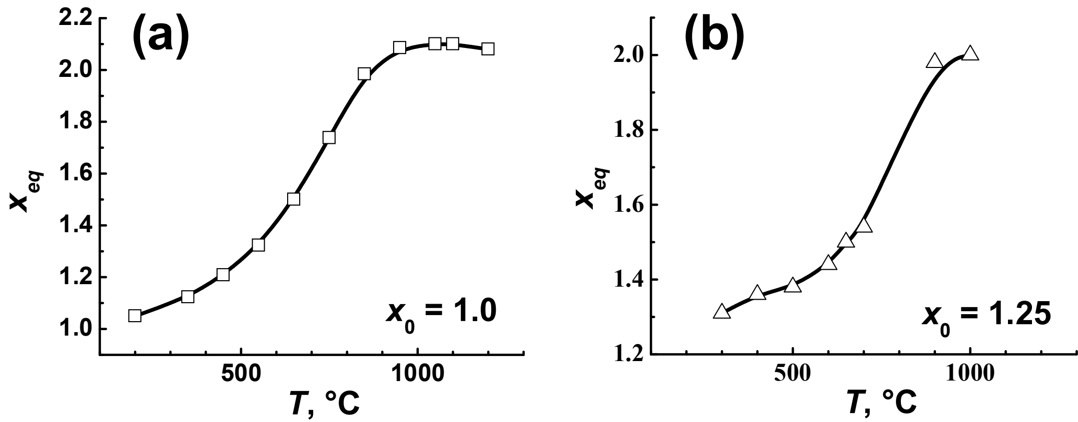

FIGURE 2.8
Experimental temperature dependences of the equilibrium stoichiometry index of resistively evaporated $SiO_{1.0}$ (a) [33] and thermal vacuum sputtered $SiO_{1.25}$ (b) [34] films

The minimum values of expression (19) determine the equilibrium states (and values of x_{eq}) of phase separated nonstoichiometric silicon oxide films for the processes, in which the formation of nanosized Si inclusions in the Si oxide matrix takes place.
Study of the dependence of the equilibrium stoichiometry index of Si oxide matrix as a function of initial stoichiometry of SiO_x film and annealing temperature requires to have the knowledge about the mathematical form of $\chi(T)$. At the moment, no exact physical model to derive this function is elaborated. Here, the temperature behavior of $\chi(T)$ is determined by comparing the equilibrium values of the stoichiometry index of Si oxide phase calculated from the minimum condition of expression (19), with the corresponding experimental saturation stoichiometry indexes of Si oxide matrix obtained after anneals of SiO_x films at different temperatures. In this work, comparison is made using the data for x_{eq} for resistively evaporated $SiO_{1.0}$ [33] and thermal vacuum sputtered $SiO_{1.25}$ films [34], the dependences of which on annealing temperature are shown in Fig. 2.8 (a) and (b), respectively. As can be seen from this figure, the transformation of Si oxide matrix into stoichiometric SiO_2 at annealing temperatures above approximately 900°C is demonstrated within the experimental error.
Fig. 2.9 shows by symbols the values of $\chi(T)$, calculated for two indicated nonstoichiometric Si oxides. For comparison, respective value from [43] (see expression (17)) recalculated per one atom in the Si / Si oxide system as $\frac{E\varepsilon_0^2}{2C_0}$ is also presented. As may be seen from this figure, this value is consistent with the theoretical values of $\chi(T)$ in the temperature range of approximately 600 to 900°C, in which the formation of amorphous Si nanoprecipitates takes place to the most extent [28, 37-42].
To make possible the investigation of the evolution of the Gibbs free energy of nano-Si / Si oxide systems with the change of x according to the expression (19), the data of $\chi(T)$ are the best fitted by exponentially decaying functions in the following form [45]:

$$\chi(T) = \chi_0 + \chi_1 \times exp\left(\frac{\varepsilon}{k_B T}\right) \qquad (20)$$

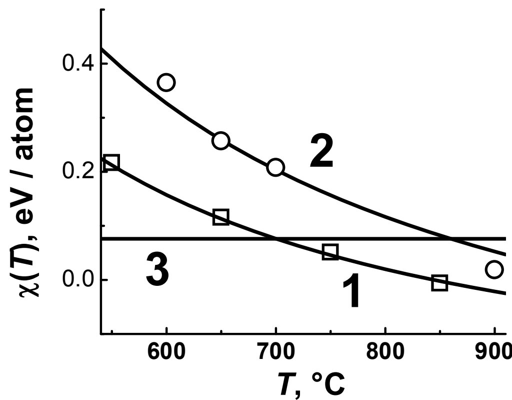

FIGURE 2.9
Values of $\chi(T)$ calculated using the experimental temperature dependences of the saturation stoichiometry index of SiO_x films (symbols) and the approximated functions (20) (lines) for the $SiO_{1.0}$ films obtained by reactive evaporation of SiO (1) [33] and $SiO_{1.25}$ films obtained by vacuum thermal sputtering (2) [34]. Line 3 represents the value $\frac{E\varepsilon_0^2}{2C_0}$ calculated on the base of the data from [43]

TABLE 2.2
Parameters characterizing the influence of the internal strain on the Gibbs free energy of the nano-Si / Si oxide systems

Sample	χ_0, eV / atom	χ_1, eV / atom	ε, eV
$SiO_{1,0}$	– 0.36	0.1	0.13
$SiO_{1,25}$	– 0.52	0.18	0.11

Respective values of the parameters χ_0, χ_1 and ε for both types of nonstoichiometric silicon oxide films mentioned above are presented in Table 2.2. The dependences of g' on x calculated by expressions (19) and (20) using the parameters χ_0, χ_1 and ε for the $SiO_{1.25}$ films as exemplary case are shown in Fig. 2.10 for different initial SiO_x compositions and temperatures (Fig. 2.10 (a) and (b), respectively). As may be seen from this figure, account of the strain contribution to the Gibbs free energy of nano-Si / Si oxide system in proposed form (18) enables to describe the experimentally observed influence of both the initial stoichiometry of Si oxide phase as well as of the annealing temperature, on the equilibrium stoichiometry index of the Si oxide matrix in the phase separated SiO_x films.
Results of the investigation carried out here show that proper behavior of the stoichiometry index of phase separated SiO_x films as a function of its initial value and annealing temperature can be explained in the framework of the thermodynamic theory of equilibrium states in Si / Si oxide systems [44] extended with additional mechanism described by the free energy term (18) [45]. Agreement between the values of $\chi(T)$ obtained from comparison with experimental data, and the value $\frac{E\varepsilon_0^2}{2C_0}$, which characterizes the internal strain in Si oxide phase according to [43], enables to reliably attribute the term (18) to the contribution to the Gibbs free energy of Si / Si oxide system

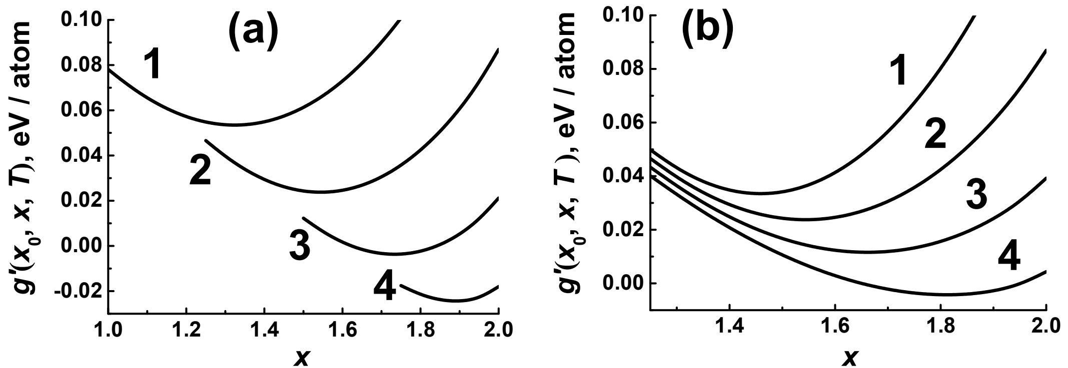

FIGURE 2.10
Theoretical dependences of the reduced Gibbs free energy on the Si oxide stoichiometry index in the a-Si / Si oxide systems calculated by expressions (19) and (20):
(a) – for different initial stoichiometry indexes of Si oxide, x_0: 1 – 1, 2 – 1.25, 3 – 1.5, and 4 – 1.75, respectively. The annealing temperature is T = 700°C.
(b) – for different annealing temperatures, T: 1 – 600, 2 – 700, 3 – 800, and 4 – 900°C, respectively. The initial silicon oxide stoichiometry is x_0 = 1.25.
All values are shifted by $\frac{1}{1+x_0}\frac{h_E - s_E T}{N_A}$ with respect to the values (19) for better visualization

of internal strain arising during phase separation of nonstoichiometric SiO_x films. Ascending character of $\chi(T)$ complies with the strain relaxation with temperature, and the parameters ε characterize the activation energy of relaxation. At the temperatures above approximately 900°C a full relaxation of strain takes place ($\chi(T) = 0$) so that the expression (18) becomes no more applicable and the (19) turns into (13). At these high temperatures SiO_x films experience complete separation with the formation of stoichiometric SiO_2 matrix composition (matrix contains also small amount of equilibrium Si, as described above), as demonstrated by the saturation behavior of x_{eq} with annealing temperature shown in Fig. 2.8. The values of $\chi(T)$ calculated for SiO_x films obtained by different technologies are also comparable. A difference between them may be related to the non-identical silicon oxide microstructure due to different processes of initial film deposition and equipment used. As supported by Fig. 2.10, appearance of internal strain in the nonstoichiometric silicon oxide films should be regarded as the principal mechanism counteracting phase separation process that defines the formation of equilibrium states in the Si nanoinclusions / Si oxide matrix systems.

Conclusion

The present review summarizes the progress achieved in the development of the thermodynamic theory of phase separation process in nonstoichiometric Si oxide (SiO_x) films during high temperature annealing. This theory is aimed at the understanding of the mechanisms of the mentioned process to enable the controlled formation of the nano-Si inclusions / Si oxide matrix composite structures for the contemporary Si based nanoelectronic device applications.
As a part of the carried out investigation, the expressions for the Gibbs free energy of silicon oxide as well as of amorphous Si / Si oxide and crystalline Si / Si oxide systems in the simplest case of

contacting bulk Si and Si oxide layers have been derived. The minimum values of the Gibbs free energy with respect to Si oxide composition determine the equilibrium states in the mentioned systems. The mechanisms promoting (driving forces) and suppressing the SiO_x phase separation have been determined according to whether the respective contributions to the Gibbs free energy descend or ascend with the increase of the stoichiometry index of separated Si oxide phase. The mechanism related to the gain in the penalty energy of $Si–O_ySi_{1−y}$ tetrahedral units composing the structure of SiO_x is the driving force of the Si and Si oxide separation. Other mechanisms such as the separation of Si in amorphous state and the transformation of configuration entropy of silicon oxide phase promote the conservation of initial SiO_x composition.
For the bulk Si / Si oxide systems, the equilibrium stoichiometry indexes of Si oxide resulted from the phase separation have been found not to depend on the initial silicon oxide stoichiometry and to decrease with temperature, which complies with the solubility limit concept of Si in SiO_2. The solubility limits of Si in SiO_2 in equilibrium with amorphous and crystalline Si have been determined, in agreement with available experimental data.
In addition, the expression for the Gibbs free energy has been modified for the case of the observed experimentally formation of nanosized Si inclusions in the Si oxide matrix during phase separation of nonstoichiometric Si oxide films. We have demonstrated the role of internal strain associated with the atom redistribution, on the equilibrium states in the case of nano-Si formation. Modification of initial expression for the Gibbs free energy of Si / Si oxide systems by adding the strain contribution enables to explain the experimentally observed dependence of the equilibrium stoichiometry index of Si oxide phase on its initial value and annealing temperature. The related to strain free energy contribution decreases with annealing temperature due to the strain relaxation and can be described by exponentially decaying function of temperature. Appearance of internal strain should be regarded as the principal mechanism that counteracts phase separation and, together with the driving force, defines the equilibrium states of the phase separated nano-Si / Si oxide systems.

References

1. M. J. O’Leary and J. H. Thomas III, J. Vac. Sci. Technol. A **5**, 106 (1987).
2. G. Hassand and C. D. Salzberg, J. Opt. Soc. **44**, 181 (1954).
3. *The physics and chemistry of SiO_2 and the $Si–SiO_2$ interface*, ed. by C. R. Helms and B. E. Deal (Plenum Press, New York, 1988).
4. A. Irrera, G. Franzò, F. Iacona, A. Canino, G. Di Stefano, D. Sanfilippo, A. Piana, P. D. Fallica, and F. Priolo, Physica E **38**, 181 (2007).
5. Zh. Yuan, A. Anopchenko, N. Daldosso, R. Guider, D. Navarro-Urrios, A. Pitanti, R. Spano, and L. Pavesi, Proc. IEEE **97**, 1250 (2009).
6. M. Wang, A. Anopchenko, A. Marconi, E. Moser, S. Prezioso, L. Pavesi, G. Pucker, P. Bellutti, and L. Vanzetti, Physica E **41**, 912 (2009).
7. R. J. Walters, G. I. Bourianoff, and H. A. Atwater, Nat. Mater. **4**, 143 (2005).
8. S. Tiwari, F. Rana, H. Hanafi, A. Hartstein, E. F. Crabbé, and K. Chan, Appl. Phys. Lett. **68**, 1377 (1996).
9. D. Tsoukalas, P. Dimitrakis, S. Kolliopoulou, and P. Normand, Mater. Sci. Eng. B **124-125**, 93 (2005).

10. R. F. Steimle, R. Muralidhar, R. Rao, M. Sadd, C. T. Swift, J. Yater, B. Hradsky, S. Straub, H. Gasquet, L. Vishnubhotla, E. J. Prinz, T. Merchant, B. Acred, K. Chang, and B. E. White Jr., Microelectronics Reliability **47**, 585 (2007).
11. S. Das Sarma, R. de Sousa, X. Hu, and B. Koiller, Solid State Commun. **133**, 737 (2005).
12. T. Shimizu-Iwayama, S. Nakao, and K. Saitoh, Appl. Phys. Lett. **65**, 1814 (1994).
13. T. P. Chen, Y. Liu, C. Q. Sun, M. S. Tse, J. H. Hsieh, Y. Q. Fu, Y. C. Eiu, and S. Fung, J. Phys. Chem. B **108**, 16609 (2004).
14. S. Furukawa and T. Miyasato, Phys. Rev. B **38**, 5726 (1988).
15. S. Hayashi, T. Nagared, Y, Kanzawa, and K. Yamamoto, Jpn. J. Appl. Phys. **32**, 3840 (1993).
16. Li. You, C. L. Heng, S. Y. Ma, Z. C. Ma, W. H. Zong, Zh. Wu, and G. G. Qin, J. Cryst. Growth **212**, 109 (2000).
17. S. Zhang, W. Zhang, and J. Yuan, Thin Solid Films **326**, 92 (1998).
18. H. Takagi, H. Ogawa, Y. Yamazaki, A. Ishizadi, and T. Nakagiri, Appl. Phys. Lett. **56**, 2379 (1990).
19. F. N. Timofeev, A. Aydinli, R. Ellialtioglu, K. Turkoglu, M. Gure, V. N. Mikhailov, and O. A. Lavrova, Solid State Commun. **95**, 443 (1995).
20. S. Veprek, Thin Solid Films **297**, 145 (1997).
21. Zh. Ma, X. Liao, J. He, W. Cheng, G. Yue, Y. Wang, and G. Kong, J. Appl. Phys. **83**, 7934 (1998).
22. F. Iacona, G. Franò, and C. Spinella, J. Appl. Phys. **87**, 1295 (2000).
23. Z. H. Hu, Nature (London) **378**, 258 (1995).
24. S. Hayashi, S. Tanimoto, M. Fujii, and K. Yamamoto, Superlattices Microstruct. **8**, 13 (1990).
25. K. Murakami, T. Suzuki, T. Makimura, and M. Tamura, Appl. Phys. A: Mater. Sci. Process. **69**, S13 (1999).
26. U. Kahler and H. Hofmeister, Appl. Phys. Lett. **75**, 641 (1999).
27. U. Kahler and H. Hofmeister, Opt. Mater. **17**, 83 (2001).
28. H. Rinnert, M. Vergnat, and A. Burneau, J. Appl. Phys. **89**, 237 (2001).
29. T. Inokuma, Y. Wakayama, T. Muramoto, R. Aoki, Y. Kurata, and S. Hasegawa, J. Appl. Phys. **83**, 2228 (1998).
30. Y. Wakayama, T. Inokuma, and S. Hasegawa, J. Cryst. Growth **183**, 124 (1998).
31. D. Comedi, O. H. Y. Zalloum, E. A. Irving, J. Wojcik, T. Roschuk, M. J. Flynn, and P. Mascher, J. Appl. Phys. **99**, 023518 (2006).
32. M. Zacharias, J. Heitmann, R. Scholz, U. Kahler, M. Schmidt and J. Bläsing, Appl. Phys. Lett. **80**, 661 (2002).
33. D. M. Zhigunov, V. N. Seminogov, V. Yu. Timoshenko, V. I. Sokolov, V. N. Glebov, A. M. Malyutin, N. E. Maslova, O. A. Shalygina, S. A. Dyakov, A. S. Akhmanov, V. Ya. Panchenko, and P. K. Kashkarov, Physica E **41**, 1006 (2009).
34. V. A. Dan'ko, I. Z. Indutnyi, V. S. Lysenko, I. Yu. Maidanchuk, V. I. Min'ko, A. N. Nazarov, A. S. Tkachenko, and P. E. Shepelyavyi, Semiconductors **39**, 1197 (2005).
35. B. J. Hinds, F. Wang, D. M. Wolfe, C. L. Hinkle, and G. Lucovsky, J. Vac. Sci. Technol. B **16**, 2171 (1998).
36. B. J. Hinds, F. Wang, D. M. Wolfe, C. L. Hinkle, and G. Lucovsky, J. Non-Cryst. Solids **227-230**, 507 (1998).
37. V. Ya. Bratus', V. A. Yukhimchuk, L. I. Berezhinsky, M. Ya. Valakh, I. P. Vorona, I. Z. Indutnyi, T. T. Petrenko, P. E. Shepeliavyi, and I. B. Yanchuk, Semiconductors **35**, 821 (2001).
38. M. Wang, D. Yang, D. Li, Zh. Yuan, and D. Que, J. Appl. Phys. **101**, 103504 (2007).

39. D. Nesheva, I. Bineva, Z. Levi, Z. Aneva, Ts. Merdzhanova, and J. C. Pivin, Vacuum **68**, 1 (2003).
40. D. Nesheva, C. Raptis, A. Perakis, I. Bineva, Z. Aneva, Z. Levi, S. Alexandrova, and H. Hofmeister, J. Appl. Phys. **92**, 4678 (2002).
41. A. F. Leier, L. N. Safronov, and G. A. Kachurin, Semiconductors **33**, 380 (1999).
42. I. P. Lisovskyy, M. V. Voitovich, A. V. Sarikov, V. G. Litovchenko, A. B. Romanyuk, V. P. Melnik, I. M. Khatsevich, and P. E. Shepeliavyi, Ukr. J. Phys. **54**, 383 (2009).
43. A. La Magna, G. Nicotra, C. Bongiorno, C. Spinella, M.G. Grimaldi, E. Rimini, L. Caristia and S. Coffa, Appl. Phys. Lett. **90**, 183101 (2007).
44. A. Sarikov and M. Zacharias, J. Phys.: Cond. Matter **24**, 385403 (2012).
45. A. Sarikov, Solid State Commun. **179**, 39 (2014).
46. A. Sarikov, Proc. NAP **3**, 01NTF16 (2014).
47. O. Nast, Ph. D. thesis, Philipps-University Marburg, 2000.
48. E. P. Donovan, F. Spaepen, J. M. Poate, and D. C. Jacobson, Appl. Phys. Lett. **55**, 1516 (1989).
49. C. Spinella, S. Lombardo, and F. Priolo, J. Appl. Phys. **84**, 5383 (1998).
50. D. A. Porter and K. E. Easterling, *Phase transformations in metals and alloys* (CRC Press, London, 1992).
51. H. R. Philipp, J. Phys. Chem. Solids **32**, 1935 (1971).
52. G. Pérez and J. M. Samz, Thin Solid Films **416**, 24 (2002).
53. D. R. Hamann, Phys. Rev. B **61**, 9899 (2000).
54. A. Bongiorno and A. Pasquarello, Phys. Rev. B **62**, R16326 (2000).
55. V. V. Slezov, Y. Schmeltzer, and Ya. T. Tkach, Sov. Phys. – Solid States **37**, 3212 (1995).
56. S. V. Bulyarsky and V. V. Svetukhin, *Physical principles of the control over defect formation in semiconductors* (UlGU, Ulyanovsk, 2002).
57. I. P. Lisovskyy, I. Z. Indutnyy, B. N. Gnennyy, P. M. Lytvyn, D. O. Mazunov, A. S. Oberemok, N. V. Sopinskyy, and P. E. Shepelyavyi, Semiconductors **37**, 97 (2003).
58. A. Sarikov, V. Litovchenko, I. Lisovskyy, I. Maidanchuk, and S. Zlobin, Appl. Phys. Lett. **91**, 133109 (2007).
59. D. V. Tsu, G. Lucovsky, and B. N. Davidson, Phys. Rev. B. **40**, 1795 (1989).
60. A. Barranco, F. Yubero, J. P. Espinós, J. P. Holgado, A. Caballero, A. R. González-Elipe, and J. A. Mejías, Vacuum **67**, 491 (2002).
61. A. Barranco, J. A. Mejías, J. P. Espinós, A. Caballero, A. R. González-Elipe, and F. Yubero, J. Vac. Sci. Technol. A **19**, 136 (2001).
62. J. J. van Hapert, A. M. Vredenberg, E. E. van Faassen, N. Tomozeiu, W. M. Arnoldbik, and F. H. P. M. Habraken, Phys. Rev. B **69**, 245202 (2004).
63. T. Müller, K.-H. Heinig, and W. Möller, Appl. Phys. Lett. **81**, 3049 (2002).
64. A. M. Agarwal and S. T. Dunham, J. Appl. Phys. **78**, 5313 (1995).
65. K. Winer, Phys. Rev. B **41**, 12150 (1990).
66. M. Zacharias and P. Streitenberger, Phys. Rev. B **62**, 8391 (2000).
67. S. Boninelli, F. Iacona, G. Franzò, C. Bongiorno, C. Spinella, and F. Priolo, J. Phys.: Cond. Matter **19**, 225003 (2007).
68. K. Sato and K. Hirakuri, J. Appl. Phys. **100**, 114303 (2006).
69. K.-Y. Ahn, R. Stengl, T. Y. Tan, U. Gösele, and P. Smith, Appl. Phys. A **50**, 85 (1990).
70. A. Borghesi, B. Pivac, A. Sassella, and A. Stella, J. Appl. Phys. **77**, 4169 (1995).
71. J. Vanhellemont and C. Claeys, J. Appl. Phys. **62**, 3960 (1987).
72. J. Schmelzer and R. Mahnke, J. Chem. Soc., Faraday Trans. **82**, 1413 (1986).

73. M. Magomedov, Low-Dim. Systems and Surface Phys. **46**, 924 (2004).
74. H. M. Lu and Q. Jiang, J. Phys. Chem. **108**, 5617 (2004).
75. D. J. Seol, S. Y. Hu, Y. L. Li, J. Shen, K. H. Oh, and L. Q. Chen, Acta Mater. **51**, 5173 (2003).